Available online at www.sciencedirect.com
SCIENCE DIRECT®

Journal of the European Ceramic Society 24 (2004) 2935–2942
www.elsevier.com/locate/jeurceramsoc

Silver containing bioactive glasses prepared by molten salt ion-exchange

S. Di Nunzio[a,*], C. Vitale Brovarone[a], S. Spriano[a], D. Milanese[a], E. Verné[a], V. Bergo[b], G. Maina[b], P. Spinelli[b]

[a]*Materials Science and Chemical Engineering Dept., Polytechnic of Turin, C.so Duca degli Abruzzi 24, 10129, Turin, Italy*
[b]*Traumatology Orthopaedics and Occupational Medicine Dept., University of Turin, Italy*

Received 28 June 2003; received in revised form 22 October 2003; accepted 8 November 2003

Abstract

Bioactive glasses containing silver on their surface were produced by ion-exchange from dilute silver nitrate melts. This technique allowed introducing Ag^+ ions only on the surface of the base glass while maintaining its bioactivity. The ion-exchanged glasses were characterized by means of X-Ray diffraction, SEM observations and compositional analysis (EDS). The control of the Ag^+ content on the surface, as well as its diffusion profile throughout the ion-exchanged layer, was obtained by a careful choice of the ion-exchange parameters (temperature, time and silver concentration in the molten bath). A very good repeatability in the diffusion profile and in the silver concentration throughout the ion-exchanged layer was achieved. In vitro tests were performed on the ion-exchanged samples in order to verify their bioactive behavior (soaking in a simulated body fluid). On the soaked samples, the precipitation of a hydroxycarbonate apatite layer (HCAp) was investigated. The amount of released Ag^+ into simulated body fluid from the exchanged glass was detected by atomic absorption spectroscopy with heated graphite furnace (GFAAS).

Keywords: Antibacterial behaviour; Bioactivity; Glass; Ion-exchange; Molten salts; SBF; Ag

1. Introduction

It is well known that silver and its compounds show an antibacterial behavior,[1–9] due to the oligodynamic activity of Ag^+ ions.[1] Some papers[10–13] reported about in vitro and in vivo effects of electrically generated silver ions. In vivo studies[10–13] showed that the use of an anodic silver therapy is a good candidate for the treatment of chronic bone infections or burns wounds. Berger et al.[10] reported that Ag^+ ions generated at an anode with weak direct current have a bactericidal activity at low concentration without any detrimental effects upon cultured cells. The behavior of bulk silver and different coatings (PVD, electro- and electroless deposited) in physiological saline solution and calf serum, was investigated by Djokic and Burrell, by open-circuit potential measurements.[1] They concluded that the antimicrobial activity of metallic silver is related to the presence of silver oxide(s) on its surface.

On the other hand, comparative in vivo studies carried out on silver pointed out the detrimental effect of pure silver on the local microvascular system, due to the cell toxicity showed by silver ions over a certain level of concentration.[2,14,15] In vivo studies were also developed on silver-coated external fixation pins, in order to evaluate both the bacterial adhesion[3] and the clinical and microbiological effects.[4] In these works, a high ability of silver coatings to inhibit the early stages of bacterial colonization, with a good control of infections around the devices, was observed. Nevertheless, these clinical studies revealed a not negligible increase of the silver level in the blood and thus deeper evaluations of the silver coatings effectiveness should be done.

More recently, several studies have been carried out on the antimicrobial effects of some metal ions in hydroxyapatite (HAp).[16,17] In these studies the Ag^+ substituted HAp demonstrated a good antimicrobial

* Corresponding author.
E-mail address: serena.dinunzio@polito.it (S. Di Nunzio).

0955-2219/$ - see front matter © 2003 Elsevier Ltd. All rights reserved.
doi:10.1016/j.jeurceramsoc.2003.11.010

effect and, in the presence of low silver ions concentration (<20 ppm), it does not loose its biocompatibility. From these studies, it came out that a too high release of silver ions could be toxic for the human body, whereas a better control of the Ag^+ release from the material could combine excellent bacteriostatic activity and biocompatibility.

Considering glass materials some researchers focused their efforts on the preparation of titanium phosphate glasses and glass-ceramics with controlled Ag^+ exchangeability in aqueous solution.[18–20] Recently, the preparation by sol-gel method of antibacterial silica glasses[21] and 45S5 Bioglass® based bioactive glasses[22–24] containing Ag_2O was also reported.

Bioactive glasses, when in contact with body fluids, show a peculiar surface chemical reactivity, which leads to the precipitation of a hydroxycarbonate apatite layer (HCAp) on their surfaces.[25,26] This latter layer provides a strong chemical bond with the surrounding tissues. The incorporation of silver ions into a bioactive glass could be an effective way to prepare bone-bonding devices that combine bioactive properties and an inhibitory action against bacterial growth.[24]

In order to produce silver-containing bioactive glasses, the conventional melt-quenching method is not effective to assure a reproducible silver ion distribution;[21] this is the reason why up-to-date, only the sol-gel method has been proposed in literature for this purpose. However, the ionic diffusion in glasses can be successfully used aiming to modify their surface composition.[27,28] Ion exchange from molten bath was particularly studied in the last 20 years to produce optical devices (glass waveguides).[29,30]

At this regard, different silicate glasses containing sodium and potassium oxides have been investigated in literature and their exchange ability has been evaluated for several cations pairs (Cs^+, Rb^+, Li^+, K^+, Ag^+).[29] The source of the exchanging ions was a mixture of molten nitrate salts.[30,31] An excellent repeatability in the diffusion profile and in the silver concentration throughout the ion-exchanged layer was achieved.[30]

In the present research work, the ion-exchange technique was applied (for the first time) aiming to produce a bioactive glass with a silver-containing surface. The aim of this research is to propose a simple, effective and low cost technique to prepare, in a quick and reproducible way, bioactive and antibacterial biomaterials. Furthermore, this technique is particularly attractive as can be applied directly to the final devices and can be easily used on an industrial scale.

2. Experimental procedures

The glass used in this work belongs to the system SiO_2–CaO–Na_2O and will be named SCN from now on. Its molar composition is the following one: 50.0% SiO_2, 25.0% CaO, 25% Na_2O.

It is considered a bioactive glass because it develops a bonelike apatite layer on its surface when soaked in a simulated body fluid with ion concentration similar to those of human plasma.[32] The in vitro apatite-forming ability can be considered as a good screening test for the in vivo bioactivity.[33] SCN was prepared by melting the starting components (SiO_2, $CaCO_3$, Na_2CO_3) in a platinum crucible at 1600 °C for 1 h (Linn Elektronic 1800). SCN was obtained by splat cooling the melt between two copper sheets in order to avoid undesired crystallization phenomena. The as obtained glass samples were annealed at 450 °C in order to release any residual internal stress and successively polished. The time and temperature conditions of annealing were chosen on the basis of the characteristic temperatures of the glass, determined in a previous work.[34]

In order to perform the ion-exchange, specimens of about 10×10 mm^2 surface (1 mm depth) of the glass were dipped in a molten bath of $AgNO_3$ and $NaNO_3$. In the following, the used bath content will be express as

Table 1
Legend of the prepared samples, ion exchange conditions tested, silver surface concentration and thickness of the ion-exchanged layer measured on the different samples

Sample	Time (min)	Solution composition	Surface Ag concentration (wt.%)	Thickness of the surface exchanged layer (μm)
H15	15	100 mol $NaNO_3$: 5 mol $AgNO_3$ (high silver content)	56	15
H30	30		–	20
H60	60		62	28
H120	120		75	50
M15	15	100 mol $NaNO_3$: 0.5 mol $AgNO_3$ (medium silver content)	51	15
M30	30		50	17
M60	60		–	22
M120	120		60	50
M240	240		72	53
L15	15	100 mol $NaNO_3$: 0.05 mol $AgNO_3$ (low silver content)	36	13
L120	120		44	40
L240	240		46	52

molar ratio (Table 1). Different samples were prepared by modifying, step by step the ion-exchanging time and the silver nitrate concentration in the molten bath.

The silver introduction in the glass surface was obtained exchanging Na^+ for Ag^+, by an equilibrium process represented by the equation:[30]

$$Na^+_{(glass)} + Ag^+_{(melt)} = Ag^+_{(glass)} + Na^+_{(melt)}$$

Table 1 reports the 12 different exchange conditions of the glass.

The samples will be named by using a letter (H, M, L) related to the silver content in the salt bath (High, Medium or Low) followed by a number corresponding to the used ion-exchanging time (Table 1). The temperature of the molten bath was constantly set at 380 °C. This temperature was chosen according to some considerations: it is above the melting points of both $AgNO_3$ (210 °C) and $NaNO_3$ (310 °C), it can assure a good flow of the molten salts (and thus a better temperature control), it is below the characteristic temperatures of the glass ($T_g = 543$ °C, $T_x = 665$ °C) [34], so any structural modification of the bulk due to heating is avoided.

The samples were analyzed by means of X-ray diffraction (X'Pert Philips diffractometer) using the Bragg Brentano camera geometry and the Cu-K_α incident radiation, and their surface morphology and composition were assessed by scanning electron microscopy (Sem Philips 525 M) and energy dispersion spectrometry (EDS Philips-EDAX 9100). In particular, for each sample, the silver surface concentration was detected as well as the thickness of the ion-exchanged layer. A silver content around 3–5%$_{wt}$ was chosen as the lower limit of the ion-exchanged layer.

Furthermore, a micro-indentation test was conduced in order to verify if the introduction of silver in the surface layer causes modifications of its mechanical properties. A load of 100 g with a Vickers indentor was used.

In vitro tests were carried out by soaking the samples in SBF. The SBF used in this work is the one proposed by Kokubo and it mimics the inorganic salt composition of human physiological fluids.[32,33] Its composition is reported in Table 2. After soaking in SBF at 37 °C, for periods up to 2 months (chosen according with the observation of HAp growing on unmodified SCN), the samples were tested by means of X-Ray diffraction, SEM observation and compositional analysis (EDS), to verify the precipitation of a HAp layer on their surfaces. Ag^+ leaching tests were carried out on a set of three samples prepared at the best-assessed exchange conditions. At this purpose, three samples of the L15 series (named L15a, L15b and L15c) and three samples of the as done SCN (used as reference), each of them of the same size and surface area (100 mm^2), were soaked into 25 ml of SBF at 37 °C up 28 days. GFAAS analyses were periodically performed by spiking 1 ml of SBF from the soaking solutions. For comparative purposes also the pure SBF (without any sample inside) was analyzed.

Table 2
Simulated body fluid according with Kokubo composition

Ion	mM / l	Salt	g/l
Na^+	142.0	KCl	0.224
K^+	5.0	$CaCl_2$	0.2775
Ca^{++}	2.5	$MgCl_2{\cdot}6H_2O$	0.305
Mg^{++}	1.5	NaCl	7.99
Cl^-	147.8	$NaHCO_3$	0.353
HCO_3^-	4.2	$K_2HPO_4{\cdot}3H_2O$	0.288
HPO_4^-	1.0	Na_2SO_4	0.07
SO_4^-	0.5	TRIS[a]	6.057

[a] Tri-hydroxymethil-methil-amine: $(HOCH_2)_3CNH_2$.

3. Results and discussion

XRD analyses were performed to verify if the ionic exchange process induced any crystallization process of the glass. Furthermore, XRD analysis also allowed verifying the eventual presence of a metallic silver phase. Fig. 1 reports the XRD patterns of samples L240 (Fig. 1a), H15 (Fig. 1b) and H120 (Fig. 1c). For the used low bath concentration, the amorphous structure of the glass was retained in every sample, even for long ion-exchanging times (L240). On the other hand, on the samples prepared by using the high bath concentration (series H) the diffraction peaks of metallic silver were detected as well as the amorphous halo. The presence of metallic silver was found for every sample of series H. Furthermore, for ion-exchanging times longer than 15 min, the crystallization of $Na_2Ca_2Si_3O_9$ took place. This crystalline phase was already found when we previously induced the crystallization of SCN and it was stated that it does not cause any depletion of the material bioactivity.[34–37]

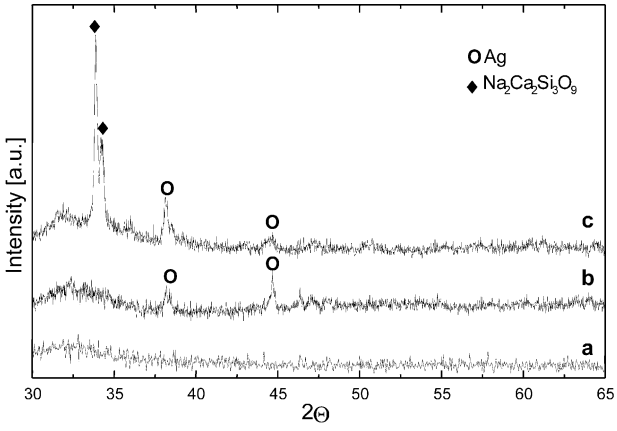

Fig. 1. X-ray diffraction patterns obtained on a L240 (a), H15 (b) and H120 (c) samples.

For series M, the presence of silver crystals has been detected for ion-exchanging times higher than 60 min. Yet, for this latter series, the crystallization of $Na_2Ca_2Si_3O_9$ didn't take place, not even for the longest ion-exchanging times (M120 and M240).

Silver crystals can be considered responsible of the crystallization of the amorphous matrix well below the T_g, as already reported in literature.[38,39]

These results assess that by modifying the ion-exchanging parameters, is possible to tailor the final surface structure of these biomaterials.[39]

The silver surface concentration detected via punctual compositional analysis on the ion-exchanged samples is reported in Table 3. As predictable, the silver surface content is both dependent on the ion-exchanging time and on the bath concentration and steadily increases with them. More precisely, for each of the three different bath concentrations (H, M, L) an almost linear trend of the silver surface concentration versus the ion-exchanging time was found (Fig. 2a).

The surface silver content can be remarkably lowered by diluting the silver concentration in the bath, as shown in table 1. At fixed times (15 min and 120 min), the silver surface content is correlated to the bath concentration by a logarithmic trend (Fig. 2b). The final silver content for the samples obtained using "short" ion-exchanging times (15–30–60 min) didn't show any remarkable difference. For this reason, samples of L series were ion-exchanged only for one "short" time (15 min) and for 2 "long" times (120 min and 240 min).

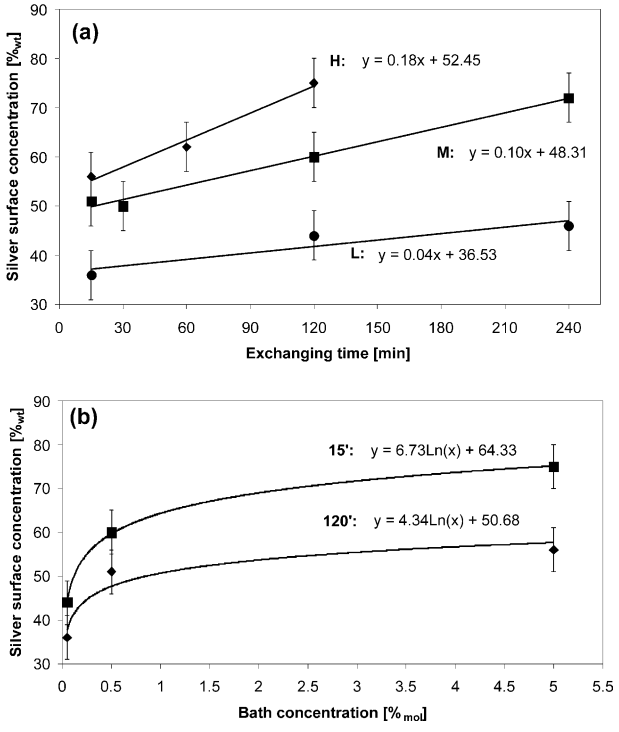

Fig. 2. Silver surface concentration vs. exchanging time (a) and vs. bath concentration (b).

However, as can be observed in Table 1, the ion-exchanging time showed a remarkable effect on the total thickness of the ion-exchanged layer, showing a linear increase of it with the processing time. In fact, for the three tested bath concentrations, the ion-exchanged layer profiles are analogous, beginning with a thickness of approximately 15 μm for the shortest time (15 min) and ending with an ion-exchange depth of about 50 μm for the highest time.

Amorphous SCN is a bioactive material and thus we focused our efforts on series L samples which didn't show any crystallization phenomena. For the above mentioned reason, on the lower bath concentration series of samples, we carried out a more accurate study of the composition profiles.

At this purpose, Fig. 3 depicts the Na and Ag concentration profiles for series L samples. As can be observed, L15 profiles show a higher slope compared to the ones found for L120 and L240 samples. This difference can be related to the shorter ion-exchanging time and thus to the correspondent limited ions diffusion path. Samples L120 and L240 showed a more gradual

Table 3
Amount (mg) of introduced Ag into different samples belonging to the low silver content series

Sample	Surface area [mm^2]	Glass weight (mg)[a]	Ag weight (mg)[b]	Ag/glass ($\%_w$)
L15a	100	*252.9* 253.8	1.144	0.45
L15b	100	*287.1* 288.6	1.906	0.66
L15c	100	*212.0* 212.8	1.017	0.48

[a] The weight indicated in *Italic font* refers to the sample before exchange (wt_{before}). The one indicated in Regular font refers to the sample after the exchange (wt_{after}).

[b] The amount of Ag^+ introduced in the glass was estimated by difference between the sample weight before and after the exchange, corrected for the atomic weight (aw) of Ag and Na, by the following formula: g Ag in the glass $= [(wt_{before} - wt_{after})/(aw^{Ag} - aw^{Na})] \cdot aw^{Ag}$.

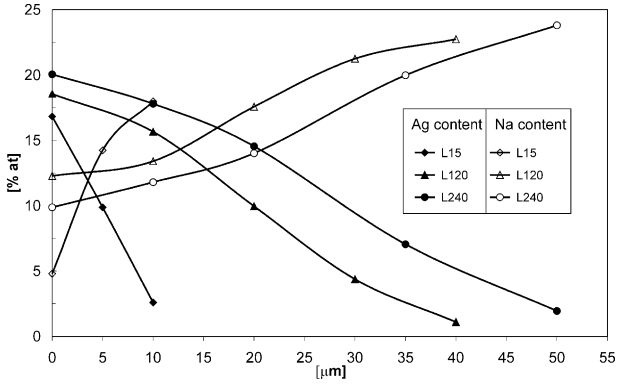

Fig. 3. Profile of the silver and sodium contents versus the surface distance detected on the samples prepared by using the lowest saline bath (L series).

modification in the ions (Ag^+ and Na^+) profiles and thus they reflect a situation closer to the equilibrium one. Considering each sample, a complementary trend of the Na^+ and Ag^+ profiles can be observed. This latter observation, confirmed that the ions involved by the ion-exchange process are Na^+ and Ag^+. Table 3 reports the amount (mg) of introduced Ag into different samples belonging to the low silver content series: the global content of silver in the glass is very low (the maximum value is $0.66\%_w$) if considering the entire mass, but it must be underlined that almost all Ag^+ ions are concentrated on glass surface.

In Fig. 4, a back-scattered micrograph of sample H15 is reported. The lighter area in the right side of the picture corresponds to the ion-exchanged layer and a constant thickness of it can be observed all over the sample. The surface homogeneity all over the samples proves that the chosen technique is suitable for the proposed aims. The micro-indentation test on the ion exchanged sample shows two cracks that propagate, from the indent corners, parallel to the surface (Fig. 5a), revealing a compression state (that as known improves mechanical resistance of the surface) due to the introduction of silver ions in the surface layer. In fact Ag^+ ions have larger size than Na^+ ones. In the bulk of the ion-exchanged sample, as well as in the unexchanged one, the indent has not preferential ways of propagation (Fig. 5b).

The bioactivity of the obtained glasses has been studied by means of in vitro tests, in order to investigate the influence of the silver presence on their surface properties. The samples were soaked in SBF for different times and then their surfaces were analysed by means of XRD and SEM-EDS analysis.

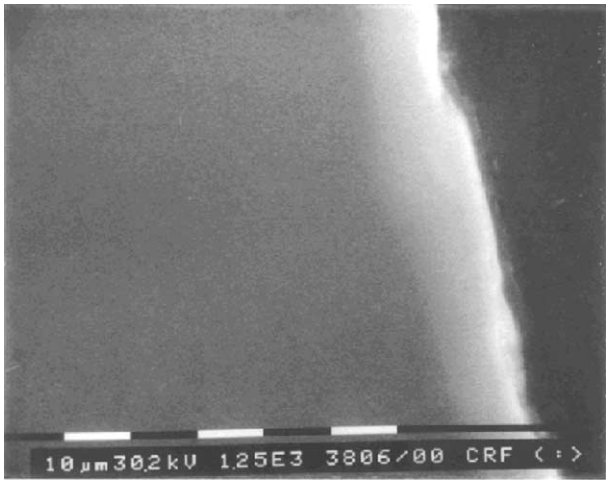

Fig. 4. Micrograph obtained by observing the cross section of a H15 sample (Backscattering signal). The surface layer, exposed to the ion exchange treatment, is evident on the right of the image as a brighter region.

For comparison purposes the same analyses were performed also on unmodified SCN glass. After 1 month soaking in SBF only a thin silica gel layer is detected by XRD analysis (the amorphous halo of silica gel, at about 20°, appears beside the halo of the glass, at about 32°) and SEM observations on the glass surface. After 2 months dipping in the solution, XRD patterns indicate the formation of a thicker layer of silica gel (only the halo at 20° is still present), SEM observation shows the presence of small agglomerates of HAp and EDS analysis confirmed an enrichment in Ca and P content on the surface.

The presence of copious AgCl crystals was observed, after soaking in SBF, on all the samples of H series. These crystals are characterized by a cubic shape with a dimension of some micrometers and cover most of the samples surface. No evidence of Ca enrichment and P presence as well as any apatite precipitation was found on these samples, not even after 2 months of soaking. So, it can be concluded that the bioactive behaviour of glassy SCN is strongly affected by the deep chemical modification of the surface induced by the ion-exchange

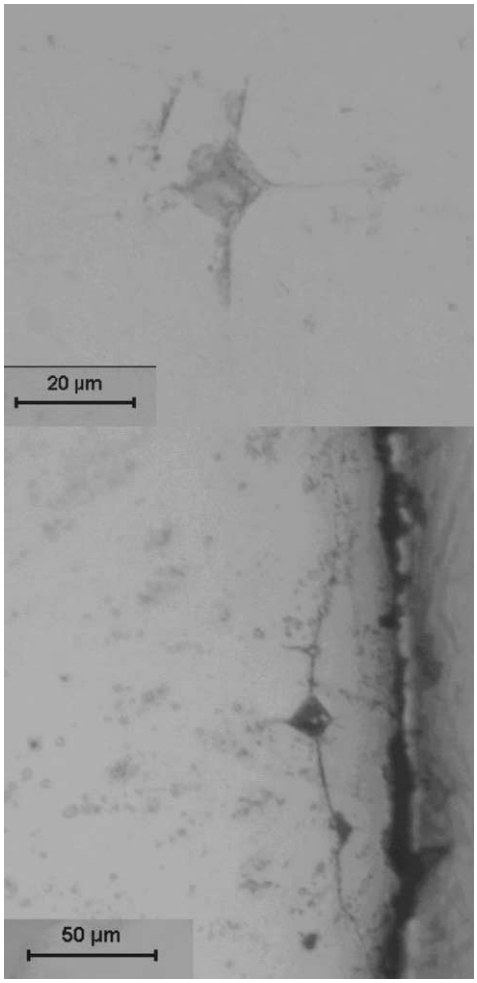

Fig. 5. Micro-indentations: (a) on SCN sample and (b) on L120 sample at about 30 µm from the surface; microindentor loaded with 100 g.

treatment performed in severe conditions (high silver content in the bath). On the contrary, both M and L series showed bioactive properties. The analysis of their surfaces put in evidence both the presence of P and Ca enrichment. Furthermore, precipitated apatite crystals were observed on these samples as shown by the micrograph reported in Fig. 6. The presence of AgCl crystals was observed on every sample. This is probably due to the quite low solubility of AgCl and to its fast precipitation on the surface during the first stage of soaking. It can be noted that generally, the apatite crystal agglomerates covered the AgCl cubic phase. Fig. 7 reports a magnification of hydroxyapatite agglomerate on sample L15 showing the typical globular morphology of precipitated hydroxyapatite. The apatite crystalline structure couldn't be investigated by XRD analysis because of the overlapping of AgCl diffraction peaks.

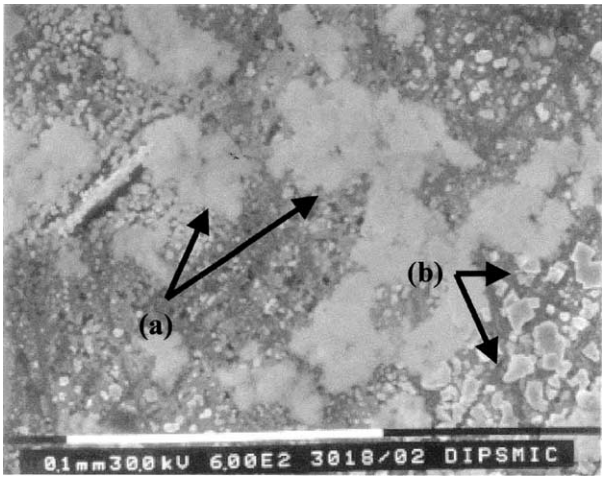

Fig. 6. Micrograph representing hydroxyapatite (a) and AgCl crystals (b) formed on the surface of a L120 sample after soaking in SBF for 2 months (secondary electron signal).

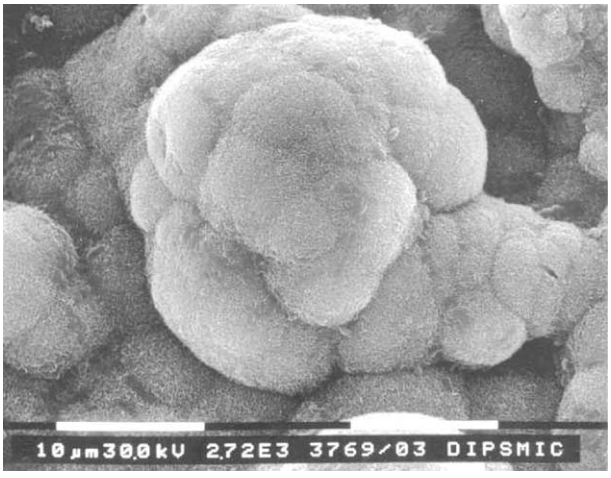

Fig. 7. Morphology of hydroxyapatite crystals grown on a L15 sample after 28 days soaking in SBF.

The effect of different ion-exchanging times was investigated by comparing L series samples, as shown in Fig. 8 where EDS analyses performed at constant low magnification were reported. By observing Fig. 8a, it is

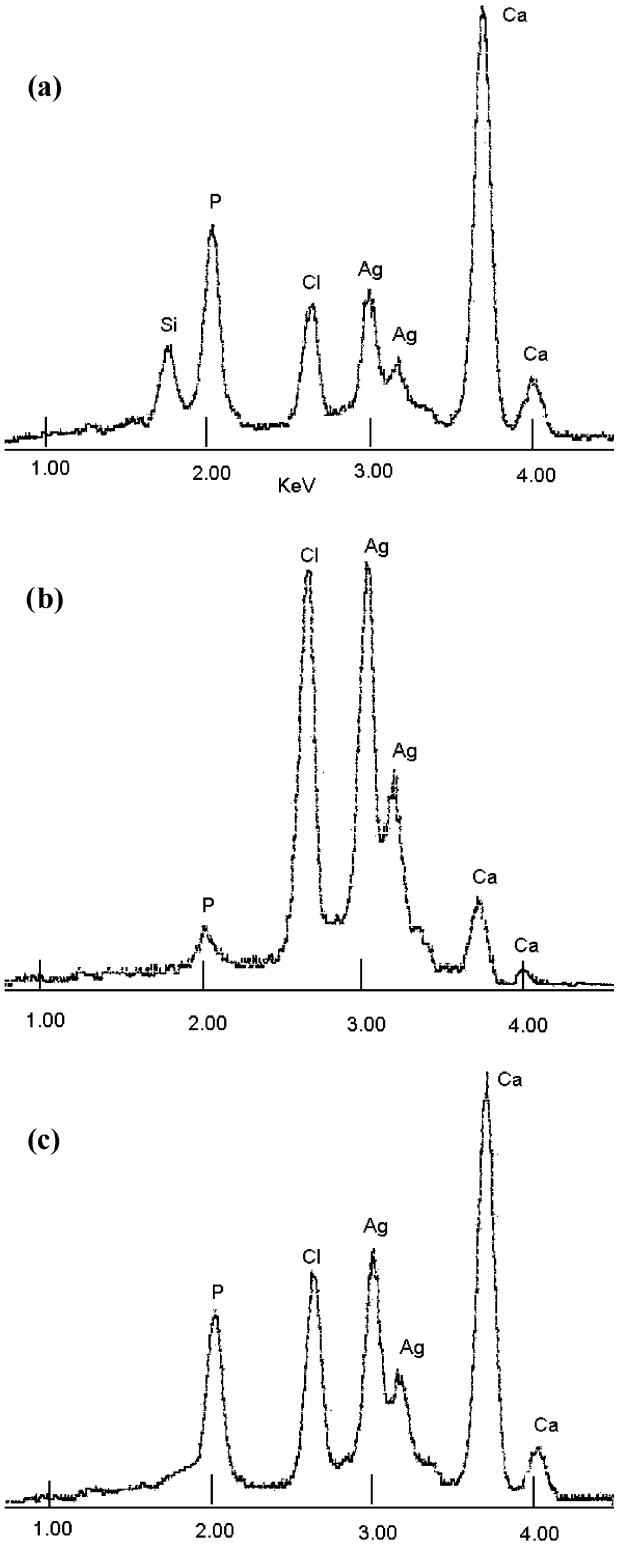

Fig. 8. EDS analysis performed on a L15 sample soaked for 28 days in SBF (layer a), on a L240 sample soaked for 1 (layer b) and 2 months (layer c) in SBF.

evident that on L15 sample, the Ca and P content is high, even after only 28 days in SBF.

Furthermore the Ca/P molar ratio measured on L15 sample is close to 1.67, the characteristic value for HAp. On the other hand, the L240 sample showed a lower bioactive ability, as can be observed by comparing Ca/P and Ag/Cl peaks intensity among the different analyses (Fig. 8b and 8c). It must be also underlined that the Ca and P content on the surface of L240 sample, after two moths soaking, is lower than that of L15 sample after only one month soaking.

The leaching tests performed on the pure SBF and on the solution in contact to the as done SCN revealed negligible amounts of Ag (probably due to raw materials impurity). The values were all in the range 1.07–3.27 μg/l; the detectable limit was 0.2 μg/l.

The solution in contact to the L15 samples revealed a not negligible release of Ag^+ during the first hours of soaking (Fig. 9). This feature is in accordance to the morphological and microstructural results, which evidenced the almost immediate AgCl precipitation on the glass surface. The precipitation of AgCl does not affect the release of a moderate amount of Ag^+, which will be responsible of the antibacterial effect. An immediate release of Ag^+ ions is a good result, since the bacteriostatic effect should take place immediately after the material implant. The maximum value of global released Ag^+ (19 $\mu g/mm^2$) is well below the critical level of citotoxicity reported in literature.[14,15,40] However, great attention should be paid to the role of the precipitated AgCl on cytotoxicity. For these reasons future efforts will be focused on a complete cytotoxicity and antibacterial evaluation of the proposed biomaterial, taking into account the possibility of further lowering the Ag content on the glass surface by a proper calibration of the exchange conditions.

4. Conclusions

The molten salts ion-exchange technique is an effective way to produce bioactive glasses with silver-containing surfaces. It is a simple and low cost technique and allows preparing, in a quick and reproducible way, bioactive materials with antibacterial properties. By a proper calibration of the ion-exchanging parameters we could tailor the final structure and the surface composition of the proposed biomaterial while maintaining its bioactive behavior and producing a silver-containing surface with a capability of silver ion release below the critical level of citotoxicity. This means that by using low silver concentration in the saline bath and low ion-exchanging time, we were able to introduce silver on the glass surface while maintaining its bioactivity and producing a potential bacteriostatic and medically safe material.

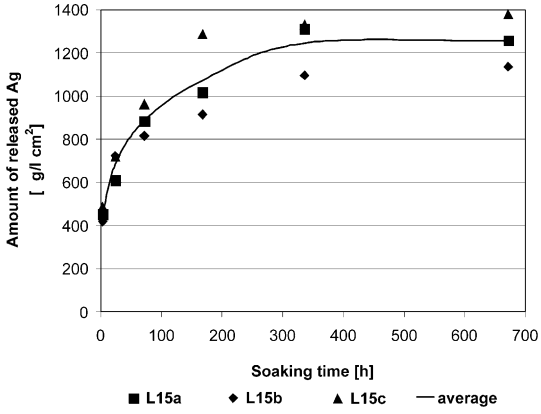

Fig. 9. Amounts of Ag^+ ions released into SBF from ion exchanged SCN glass. (■ L15a, ◆ L15b, • L15c,—average).

Furthermore, the proposed method can be applied directly to the final devices and can be easily used on an industrial scale.

Acknowledgements

Prof. M. Ferraris is kindly acknowledged for her support. The Fiat Research Center of Orbassano (Torino, Italy) is kindly acknowledged for SEM facilities. This research work was partially funded by Polytechnic of Turin ("*Progetto Giovani Ricercatori*").

References

1. Djokić, S. S. and Burrell, R. E., Behaviour of silver in physiological solutions. *J. Electrochem. Soc*., 1998, **145**(5), 1426–1430.
2. Kraft, C. N., Hansis, M., Arens, S., Menger, M. D. and Vollmar, B., Striated muscle microvascular response to silver implants: a comparative in vivo study with titanium and stainless steel. *J. Biomed. Mater. Res*., 2000, **49**, 192–199.
3. Wassall, M. A., Santin, M., Isalberti, C., Cannas, M. and Denyer, S. P., Adhesion of bacteria to stainless steel and silver-coated orthopaedics external fixation pins. *J. Biomed. Mater. Res*., 1997, **36**, 325–330.
4. Massè, A., Bruno, A., Bosetti, M., Biasibetti, A., Cannas, M. and Gallinaro, P., Prevention of pin track infection in external fixation with silver coated pins: clinical and microbiological results. *J. Biomed. Mater. Res. (Appl. Biomater.)*, 2000, **53**, 600–604.
5. Stanislawsky, L., Daniau, X., Lautiè, A. and Goldberg, M., Factors responsible for pulp cell cytotoxicity induced by resin-modified glass ionomer cements. *J. Biomed. Mater. Res. (Appl. Biomater.)*, 1999, **48**, 277–288.
6. Yoshida, K., Tanagawa, M. and Atsuta, M., Characterization and inhibitory effect of antibacterial dental resin composites incorporating silver-supported materials. *J. Biomed. Mater. Res*., 1999, **47**, 516–522.
7. Westenberg, D., Fighting infections with glass. In: *Proceedings of the 100th General Meeting of the American Society for Microbiology*, Los Angeles, ASM, 21–25 May 2000.
8. Kumon, H., Hashimoto, H., Nishimura, M., Monden, K. and Ono, N., Catheter-associated urinary tract infections: impact of catheter materials on their management. *Int. J. Antimicrobial Agents*, 2001, **17**, 311–316.

9. Feng, Q. L., Wu, J., Chen, G. Q., Cui, F. Z., Kim, T. N. and Kim, J. O., A mechanistic study of the antibacterial effect of silver ions on *Escherichia coli* and *Staphylococcus aureus*. *J. Biomed. Mater. Res.*, 2000, **52**, 662–668.
10. Berger, T. J., Spadaro, J. A., Chapin, S. E. and Becker, R. O., Electrically generated silver ions: quantitative effects on bacterial and mammalian cells. *Antimicrobial Agents and Chemotherapy*, 1976, **9**(2), 357–358.
11. Becker, R. O. and Spadaro, J. A., Treatment of orthopaedic infections with electrically generated ions. *The J. Bone and Joint Surgery*, 1978, **60**(7), 871–881.
12. Webster, D. A., Spadaro, J. A., Becker, R. O. and Kramer, S., Silver anode treatment of chronic osteomyelitis. *Clinical Orthopaedics and Related Research*, 1981, **161**, 105–114.
13. Chu, C., McManus, A. T., Pruitt, B. A. Jr. and Mason, A. D. Jr., Therapeutics effects of silver nylon dressings with weak direct current on *Pseudomonas aeruginosa*-infected burn wounds. *The J. Trauma*, 1988, **28**(10), 1488–1492.
14. Wataha, J. C., Lockwood, P. E. and Schedle, A., Effect of silver, copper, mercury and nickel on cellular proliferation during extended, low-dose exposures. *J. Biomed. Mater. Res.*, 2000, **52**, 360–364.
15. Williams, R. L., Doherty, P. J., Vince, D. G., Grashoff, G. J. and Williams, D. F., The biocompatibility of silver. *Critical Reviews in Biocompatibility*, 1989, **5**(3), 221–243.
16. Kim, T. N., Feng, Q. L., Kim, J. O., Wu, J., Wang, H., Chen, G. C. and Cui, F. Z., Antimicrobial effects of metal ions (Ag^{+}, Cu^{2+}, Zn^{2+}) in hydroxyapatite. *J. Mater. Sci.: Mater. In Med.*, 1998, **9**, 129–134.
17. Feng, Q. L., Cui, F. Z., Kim, T. N. and Kim, J. W., Ag-substituted hydroxyapatite coatings with both antimicrobial effects and biocompatibility. *J. Mater. Sci. Lett.*, 1999, **18**, 559–561.
18. Hosono, H. and Abe, Y., Silver ion selective lithium titanium phosphate glass-ceramic cation exchanged and its application to bacteriostatic materials. *Materials Research Bulletin*, 1994, **29**(11), 1157–1162.
19. Kasuga, T., Kume, H. and Abe, Y., Porous glass-ceramics with bacteriostatic properties in silver-containing titanium phosphates: control of release of silver ions from glass-ceramics to aqueous solution. *J. Am. Ceram. Soc.*, 1997, **80**(3), 777–780.
20. Kasuga, T., Nogami, M. and Abe, Y., Titanium phosphate glass-ceramics with silver ion exchangeability. *J. Am. Ceram. Soc.*, 1999, **82**(3), 765–767.
21. Kawashita, M., Tsuneyama, S., Miyaji, F., Kokubo, T., Kozuka, H. and Yamamoto, K., Antibacterial silver-containing silica glass prepared by sol-gel method. *Biomaterials*, 2000, **21**, 393–398.
22. Bellantone, M., Coleman, N. J. and Hench, L. L., Bacteriostatic action of a novel four-component bioactive glass. *J. Biomed. Mater. Res.*, 2000, **51**, 484–490.
23. Bellantone, M., Coleman, N. J. and Hench, L. L., A novel sol-gel derived glass featuring antibacterial properties. In *Bioceramics. Key Engineering Materials vol 192–195*, ed. S. Giannini and A. Moroni. Trans Tech Publ Ltd, Totton, UK, 2001, pp. 597–600.
24. Bellantone, M. and Hench, L. L., Bioactive behaviour of sol-gel derived antibacterial bioactive glass. In *Bioceramics. Key Engineering Materials vol 192–195*, ed. S. Giannini and A. Moroni. Trans Tech Publ Ltd, Totton, UK, 2001, pp. 617–620.
25. Hench, L. L., *Bioceramics. J. Am. Ceram. Soc.*, 1998, **81**(7), 1705–1728.
26. Ballarre, J., Orellano, J. C., Bordenave, C., Galliano, P. and Cerè, S., In vivo and in vitro evaluation of vitreous coatings on cobalt base alloys for prosthetics devices. *J. Non-Cry. Sol*, 2002, **304**, 278–285.
27. Wang, P. W., Zhang, L., Tao, Y. and Wang, C., Thermal behaviour of silver in ion-exchanged soda-lime glasses. *J. Am. Ceram. Soc.*, 1997, **80**(9), 2285–2293.
28. Terai, R. and Hayami, R., Ionic diffusion in glasses. *J. Non-Crystall. Solids*, 1975, **18**, 217–264.
29. Ramaswamy, R. V. and Srivastava, R., Ion-exchanged glass waveguides: a review. *J. Lightwave Techn*, 1988, **6**(6), 984–1001.
30. Steward, G. and Laybourn, P. J. R., Fabrication of ion-exchanged optical waveguides from dilute silver nitrate melts. *IEEE J.Quantum Electr.*, 1978, **QE-14**(12), 930–934.
31. Jackel, J. L., Glass waveguides made using low melting point nitrate mixtures. *Applied Optics*, 1988, **Feb. 27**(3).
32. Kim, H. M., Miyaji, F., Kokubo, T., Ohtsuki, C. and Nakamura, T., Bioactivity of Na_2O–CaO–SiO_2 glasses. *Journal of American Ceramic Society*, 1995, **78**(9), 2405–2411.
33. Fujibayashi, S., Neo, M., Kim, H. M., Kokubo, T. and Nakamura, T., A comparative in vivo bone ingrowth and in vitro apatite formation on Na_2O–CaO–SiO_2 glasses. *Biomaterials*, 2003, **24**, 1349–1356.
34. Verné, E., Bona, E., Bollosi, A., Vitale Brovarone, C. and Appendino, P., Na_2O–CaO–SiO_2 glass-ceramic matrix biocomposites. *J. Mat. Sci.*, 2001, **36**, 2801–2807.
35. Verné, E., Vitale Brovarone, C. and Milanese, D., Glass-matrix biocomposites: synthesis and characterisation. *J. Biom. Mater. Res (Applied Biomater)*, 2000, **53**, 408–413.
36. Vitale Brovarone, C., Di Nunzio, S., Bretcanu, O. and Verné, E., Macroporous glass-ceramic materials with bioactive properties, *J. Mater. Sci. Mater. Med.*, 2004, **15**, 1–9.
37. Peitl, O., Zanotto, E. and Hench, L. L., Highly bioactive P_2O_5 Na_2O CaO SiO_2 glass-ceramics. *J. Non-Cry Sol*, 2001, **292**, 115–126.
38. Takada, H., Yano, T., Yasumori, A., Shibata, S. and Yamane, M., Ion-exchanged induced crystallization of a glass below Tg. In *Nucleation and crystallization of glasses and liquids*, ed. M. C. Weinberg. American Ceramic Society, 1993.
39. Yano, T., Azegami, K., Shibata, S. and Yamane, M., Chemical state of oxygen in Ag^{+}/Na^{+} ion-exchanged sodium silicate glass. *J. Non-Cry. Sol.*, 1997, **222**, 94–101.
40. Dowling, D. P., Donnely, K., McConnell, M. L., Eloy, R. and Arnaud, M. N., Deposition of anti-bacterial silver coatings on polymeric substrates. *Thin Solid Films*, 2001, **398–399**, 602–606.